

Spin accumulation in lateral semiconductor superlattices induced by a constant electric field

P. Kleinert

Paul-Drude-Institut für Festkörperelektronik, Hausvogteiplatz 5-7, 10117 Berlin, Germany

V. V. Bryksin

Physical Technical Institute, Politeknicheskaya 26, 194021 St. Petersburg, Russia

O. Bleibaum

Institut für Theoretische Physik, Otto-von-Guericke Universität Magdeburg, PF4120, 39016 Magdeburg, Germany

(Received 9 August 2005; published 8 November 2005)

The electric-field dependence of the spin accumulation in strongly coupled lateral superlattices subject to Rashba spin-orbit interaction is studied by the density-matrix approach. At low fields, the spin accumulation depends linearly on the electric field. In this field regime, the magnitude of the homogeneous magnetization is larger in the lateral superlattice than in the corresponding two-dimensional electron gas. The magnetization exhibits a maximum as a function of the electric field. In the region of Wannier-Stark localization, the field-induced magnetization decreases with increasing electric field strength. Field-mediated resonant-tunneling transitions between different spin states manifest themselves in a spin depolarization.

DOI: [10.1103/PhysRevB.72.195311](https://doi.org/10.1103/PhysRevB.72.195311)

PACS number(s): 72.25.Pn, 72.20.Ht, 85.75.-d

I. INTRODUCTION

Manipulating the spin degree of freedom by electrical means for electronic device applications is one of the main objectives in the fast developing field of spin electronics. In this context, it would be attractive to induce a nonequilibrium magnetization exclusively by the application of electric fields. In the literature, two mechanisms are widely discussed, which permit the generation of a magnetization by an electric field in semiconductors with spin-orbit interaction: The spin-Hall effect (see, e.g., Refs. 1–6) and the spin accumulation.^{7–13} In the spin-Hall effect, a transverse non-equilibrium magnetization is induced at the sample boundaries of a two-dimensional electron gas in the presence of an electric field. In contrast, the spin accumulation, which is due to a charge current flowing through a two-dimensional electron gas, is characterized by a homogeneous magnetization. This mechanism of spin polarization results under nonequilibrium conditions from the spin-orbit interaction, which gives rise to an effective magnetic field.

Whereas the spin-Hall effect also occurs in systems, in which the spin-orbit scattering is provided by impurities, we expect that the spin accumulation is only observed in systems without structural or bulk inversion symmetry. Such systems differ from two-dimensional electron gases with spin-orbit scattering due to impurities in that the momentum of the particles is coupled to their spin. Accordingly, a non-equilibrium magnetization can arise by shifting the Fermi surface in an appropriate way, as it is done by means of an electric or by coupled electric and magnetic fields. Thus, the spin accumulation is a kinetic analogy of the magnetoelectric effect in antiferromagnetic insulators and can be regarded as complementary to the recently discovered spin-galvanic effect.¹⁴

The spin accumulation has been treated in the literature only in the linear electric field regime for semiconductor heterostructures with Rashba spin-orbit interaction. It has been

shown that in this regime the magnetization is directly proportional to the magnitude of the Rashba coupling strength and to the momentum relaxation time. The spin-polarization itself, however, is rather small so that large electric fields are needed to produce measurable magnetizations. This raises the question, whether the results derived for the linear field region still apply to the experimental situation and to what extent the magnetization can be increased by increasing the electric field and by changing the experimental setup.

It is the main objective of this paper to generalize previous approaches of the spin accumulation, which remained within the framework of linear response theory, to the nonlinear high-electric field regime. As nonlinear field effects are more easily studied in superlattices with large Bloch frequencies $\Omega = e\mathcal{E}d/\hbar$ (with \mathcal{E} and d denoting the electric field and the superlattice period, respectively), we shall focus on such systems by exploiting methods worked out in the field of nonequilibrium carrier transport (see, e.g., Ref. 15). To be more specific, it is our aim to present a quantum-mechanical calculation of the field-induced spin accumulation for a lateral semiconductor superlattice with Rashba spin-orbit coupling and an in-plane electric field on the basis of kinetic equations for the nonequilibrium density matrix. First results based on the quasi-classical approximation have been obtained recently.¹⁶

II. BASIC THEORY

Let us treat a lateral superlattice with a strong potential modulation along the x axis as can be fabricated by the cleave-edge overgrowth technique. The tight-binding dispersion relation of this model has the form

$$\varepsilon(\mathbf{k}) = \frac{\Delta}{2}[1 - \cos(k_x d)] + \varepsilon(k_y), \quad (1)$$

where $\mathbf{k} = (k_x, k_y)$ denotes the quasi-momentum in the plane, Δ the width of the lowest miniband, and $\varepsilon(k_y) = \hbar^2 k_y^2 / 2m^*$ the

contribution to the kinetic energy for the carrier motion along the y axis, respectively. The Hamiltonian of the biased lateral superlattice with Rashba spin-orbit coupling has the form

$$H_0 = \sum_{k,\sigma} \varepsilon(\mathbf{k}) a_{k\sigma}^\dagger a_{k\sigma} + \sum_k \sum_{\sigma,\sigma'} J_{\sigma\sigma'}(\mathbf{k}) a_{k\sigma}^\dagger a_{k\sigma'} - ie\vec{\mathcal{E}} \sum_{k,\sigma} \nabla_\kappa (a_{k-\kappa/2\sigma}^\dagger a_{k+\kappa/2\sigma}) \Big|_{\kappa=0}. \quad (2)$$

where $a_{k,\sigma}^\dagger$ and $a_{k,\sigma}$ are creation and annihilation operators, respectively, for electrons with quasimomentum \mathbf{k} and spin σ . The in-plane constant electric field vector $\vec{\mathcal{E}}$ is oriented along the x axis. The field contribution to the Hamiltonian in Eq. (2) is calculated in the scalar gauge and expressed in the quasi-momentum representation.¹⁵ Note that the Hamiltonian is not diagonal due to the electric field $\vec{\mathcal{E}}$ and the Rashba spin-orbit coupling, which is described by the matrix

$$J_{\sigma\sigma'}(\mathbf{k}) = \begin{pmatrix} 0 & J_{12}(\mathbf{k}) \\ J_{12}^*(\mathbf{k}) & 0 \end{pmatrix}, \quad J_{12}(\mathbf{k}) = \alpha m^* [iv_x(\mathbf{k}) + v_y(\mathbf{k})]. \quad (3)$$

Here α denotes the Rashba spin-orbit coupling constant and $v_x(\mathbf{k})$ and $v_y(\mathbf{k})$ are the components of the drift velocity. The tight-binding dispersion relation of Eq. (1) yields

$$J_{12}(\mathbf{k}) = \alpha m^* \left(i \frac{\Delta d}{2\hbar} \sin(k_x d) + \frac{\hbar k_y}{m^*} \right). \quad (4)$$

In order to calculate the field-induced spin polarization for a system with Rashba interaction, we apply a canonical transformation that diagonalizes the Hamiltonian under zero bias ($\mathcal{E}=0$). Such a transformation has the form

$$a_{k\sigma} = \sum_\mu A_{\sigma\mu}(\mathbf{k}) b_{k\mu}, \quad \sum_\mu A_{\sigma\mu}^*(\mathbf{k}) A_{\sigma'\mu}(\mathbf{k}) = \delta_{\sigma\sigma'}, \quad (5)$$

where the matrix

$$\hat{A}(\mathbf{k}) = \frac{1}{\sqrt{2}} \begin{pmatrix} e^{-i\varphi_k/2} & e^{-i\varphi_k/2} \\ -e^{i\varphi_k/2} & e^{i\varphi_k/2} \end{pmatrix},$$

is calculated from a phase factor φ_k that depends on the quasi-momentum and which is determined by one of the following equations

$$\sin(\varphi_k) = \alpha m^* \frac{\Delta d}{2\hbar} \sin(k_x d) / J(\mathbf{k}), \quad \cos(\varphi_k) = -\alpha \hbar k_y / J(\mathbf{k}). \quad (6)$$

The function

$$J(\mathbf{k}) = \alpha m^* \sqrt{\left(\frac{\hbar k_y}{m^*} \right)^2 + \left(\frac{\Delta d}{2\hbar} \sin(k_x d) \right)^2} \quad (7)$$

is one half of the spin-mediated energy splitting, which enters our final Hamiltonian

$$H_0 = \sum_{k\mu} \varepsilon_\mu(\mathbf{k}) b_{k\mu}^\dagger b_{k\mu} - e\vec{\mathcal{E}} \sum_k d(\mathbf{k}) (b_{k1}^\dagger b_{k2} + b_{k2}^\dagger b_{k1}) - ie\vec{\mathcal{E}} \sum_{k\mu} \nabla_\kappa b_{k-\kappa/2\mu}^\dagger b_{k+\kappa/2\mu} \Big|_{\kappa=0}. \quad (8)$$

In the new basis, the model is characterized by spin dependent eigenenergies $\varepsilon_\mu(\mathbf{k}) = \varepsilon(\mathbf{k}) \mp J(\mathbf{k})$ and a dipole moment $e\mathbf{d}(\mathbf{k}) = e\nabla_k \varphi_k / 2$, which is proportional to k_y .

We are interested in calculating the quantity $f_y(\mathbf{k}) = i[f_{21}(\mathbf{k}) - f_{12}(\mathbf{k})]$ (the x and z components of the magnetization vanish even at nonzero electric fields due to symmetry arguments), where the elements of the density matrix are given by $f_{\sigma\sigma'}(\mathbf{k}) = \langle a_{k\sigma}^\dagger a_{k\sigma'} \rangle$. The quantity $f_y(\mathbf{k})$ is related to the components of the density matrix $F_{\mu\mu'}(\mathbf{k}) = \langle b_{k\mu}^\dagger b_{k\mu'} \rangle$ in the new basis by the relationship

$$f_y(\mathbf{k}) = \cos(\varphi_k) F_y(\mathbf{k}) - \sin(\varphi_k) F_z(\mathbf{k}). \quad (9)$$

Here, we used the abbreviations $F_z(\mathbf{k}) = F_{11}(\mathbf{k}) - F_{22}(\mathbf{k})$ and $F_y(\mathbf{k}) = i(F_{21}(\mathbf{k}) - F_{12}(\mathbf{k}))$. Taking into account Eq. (6), we obtain a result

$$f_y = -\alpha m^* \frac{\Delta d}{2\hbar} \sum_{k_x, k_y} \frac{\sin(k_x d)}{J(\mathbf{k})} F_z(\mathbf{k}) - \alpha \hbar \sum_k \frac{k_y}{J(\mathbf{k})} F_y(\mathbf{k}), \quad (10)$$

which consists of two quite different contributions. The first one on the right hand side of Eq. (10) survives in the low-field limit ($\mathcal{E} \rightarrow 0$) and is calculated from the diagonal elements of the density matrix $F_{\mu\mu'}(\mathbf{k})$. For a two-dimensional electron gas, this contribution has the form

$$f_y = -\sum_k \sin \varphi_k F_z(\mathbf{k}) = -\sum_k \frac{k_x}{|\mathbf{k}|} F_z(\mathbf{k}). \quad (11)$$

It is clear from this equation that only the anti-symmetric part of the distribution function $F_z(\mathbf{k})$ contributes. Quite similar to the treatment of the Boltzmann equation in the quasi-elastic limit, this quantity is calculated from the kinetic equation for the density matrix [cf. Eq. (14) in Sec. III] by adopting the constant relaxation-time approximation with respect to scattering. At zero temperature ($T=0$) and in the linear electric field regime, we obtain the solution

$$F_z(\mathbf{k}) = -\frac{e\mathcal{E}\tau_s}{\hbar} \frac{\partial}{\partial k_x} [\Theta(\varepsilon_1(\mathbf{k}) - \varepsilon_F) - \Theta(\varepsilon_2(\mathbf{k}) - \varepsilon_F)], \quad (12)$$

with ε_F and τ_s denoting the Fermi energy and an effective elastic scattering time, respectively. Carrying out the integrations over the k_x and k_y variables in Eq. (11), we obtain the analytical result

$$f_y = \frac{\alpha m^* a^2}{2\pi\hbar^2} e\mathcal{E}\tau_s, \quad (13)$$

which was derived previously⁷ for a two-dimensional electron gas with the lattice constant a . The second contribution on the right-hand side of Eq. (10) is determined by the off-diagonal components of the density matrix. This term describes quantum effects due to field-induced tunneling. Both contributions are calculated in the next section for strongly coupled lateral superlattices.

III. TRANSPORT EQUATIONS

Our calculation of the magnetization is based on kinetic equations for the density matrix $F_{\mu\mu'}(\mathbf{k})$, which is obtained from the Liouville equation that enter the one-particle Hamiltonian in Eq. (8) and scattering contributions. In the presence of an electric field and for a nondegenerate electron gas, the kinetic equations have the form¹⁵

$$\begin{aligned} & \left\{ \frac{\partial}{\partial t} - \frac{i}{\hbar}(\varepsilon_{\mu}(\mathbf{k}) - \varepsilon_{\mu'}(\mathbf{k})) + \frac{e}{\hbar}(\vec{\mathcal{E}} \cdot \nabla) \right\} F_{\mu\mu'}(\mathbf{k}|t) \\ & + \frac{i}{\hbar}(\vec{\mathcal{E}} \cdot \mathbf{d}(\mathbf{k}))[\sigma_x F(\mathbf{k}|t)]_{\mu\mu'} \\ & = \sum_{k'} \sum_{\mu_1\mu_2} (F_{\mu_1\mu_2}(k') W_{\mu_1\mu}^{\mu_2\mu'}(k', \mathbf{k}) \\ & - F_{\mu_1\mu_2}(\mathbf{k}) W_{\mu_1\mu}^{\mu_2\mu'}(\mathbf{k}, k')), \end{aligned} \quad (14)$$

where σ_x denotes the Pauli matrix and $W_{\mu_1\mu}^{\mu_2\mu'}(k', \mathbf{k})$ are transition probabilities that depend both on the electric field and the spin-orbit coupling and that refer to elastic and inelastic scattering mechanisms. In general, the solution of these equations is a formidable task that can only be solved by a numerical approach. To focus on the essential physics and for simplicity, we adopt here a simple treatment of scattering based on the relaxation-time approximation. Although this approximation inevitably lacks some features of a more realistic description, its usefulness in deriving main physical results in a qualitative manner has clearly been demonstrated. However, we want to point out that the application of the relaxation-time approximation to our model becomes more difficult because the off-diagonal elements of the transition probabilities are nonvanishing, since the quantities $A_{\sigma\mu}(\mathbf{k})$ are not orthogonal for different \mathbf{k} , i.e.

$$\sum_{\mu} A_{\sigma\mu}^*(\mathbf{k}) A_{\sigma'\mu}(\mathbf{k}') \neq 0, \quad (15)$$

for $\sigma \neq \sigma'$ and $\mathbf{k} \neq \mathbf{k}'$. Therefore, the scattering probabilities couple off-diagonal to diagonal elements of the density matrix. This coupling disappears, however, in systems with long-range scattering. We shall focus on this particular case so that the relaxation-time approximation is applicable in the conventional manner, however, with scattering times that essentially depend on the quasi-momentum \mathbf{k} . Therefore, the full solution to the problem would involve the treatment of a microscopic model for long-range scattering that allows the

calculation of the \mathbf{k} dependent scattering times. Such calculations would be too complicated for the present analytical study that is intended to demonstrate qualitative features of the nonlinear field-induced spin polarization. For simplicity, we therefore apply the constant relaxation-time approximation although this model inevitably lacks some of the features of a more realistic description of real systems. For the components of the density matrix, we obtain the set of equations

$$\begin{aligned} & \left\{ \frac{\partial}{\partial t} + \frac{e}{\hbar}(\vec{\mathcal{E}} \cdot \nabla) \right\} F_{11/22}(\mathbf{k}|t) \pm \frac{i}{\hbar}(\vec{\mathcal{E}} \cdot \mathbf{d}(\mathbf{k}))(F_{21}(\mathbf{k}|t) - F_{12}(\mathbf{k}|t)) \\ & = -\frac{1}{\tau_s}(F_{11/22}(\mathbf{k}|t) - F_{11/22}^0(\mathbf{k})), \end{aligned} \quad (16)$$

$$\begin{aligned} & \left\{ \frac{\partial}{\partial t} \mp 2\frac{i}{\hbar}J(\mathbf{k}) + \frac{e}{\hbar}(\vec{\mathcal{E}} \cdot \nabla) \right\} F_{12/21}(\mathbf{k}|t) \\ & \pm \frac{i}{\hbar}(\vec{\mathcal{E}} \cdot \mathbf{d}(\mathbf{k}))(F_{22}(\mathbf{k}|t) - F_{11}(\mathbf{k}|t)) \\ & = -\frac{1}{\tau}F_{12/21}(\mathbf{k}|t), \end{aligned} \quad (17)$$

where the upper (lower) sign refers to the equation for F_{11} (F_{22}) (the same sign convention applies to the equations for F_{12} and F_{21}). The quantities τ and τ_s are phenomenological relaxation times, and

$$F_{11/22}^0(\mathbf{k}) = \frac{1}{\exp[\beta(\varepsilon_{1/2}(\mathbf{k}) - \varepsilon_F)] + 1} \quad (18)$$

is the Fermi distribution function with ε_F denoting the Fermi energy and $\beta=1/k_B T$.

For an electric field oriented along the x axis, Eqs. (16) and (17) are solved in the Wannier-Stark representation, which is introduced by the discrete Fourier transformation¹⁷

$$F_{\mu\mu'}(\mathbf{k}) = \sum_{l=-\infty}^{\infty} e^{ilk_x d} F_{\mu\mu'}(l, k_y). \quad (19)$$

In this representation and for the steady state, Eqs. (16) and (17) take the form

$$\begin{aligned} & i\Omega F_{11/22}(l, k_y) \pm \frac{ie\mathcal{E}}{\hbar} \sum_{l_1} d_x(l-l_1, k_y)(F_{21}(l_1, k_y) - F_{12}(l_1, k_y)) \\ & = -\frac{1}{\tau_s}(F_{11/22}(l, k_y) - F_{11/22}^0(l, k_y)) \end{aligned} \quad (20)$$

and

$$\begin{aligned} & \left[\frac{1}{\tau} \mp 2\frac{i}{\hbar}J(k_y) + i\Omega \right] \tilde{F}_{12/21}(l, k_y) \\ & = \pm \frac{ie\mathcal{E}}{\hbar} \sum_{l'} d_x^{\pm}(l-l', \mathbf{k}) F_z(l', k_y), \end{aligned} \quad (21)$$

with

$$\bar{J}(k_y) = \frac{d}{2\pi} \int_0^{2\pi/d} dk_x J(\mathbf{k}). \quad (22)$$

Note that the simple solution in Eq. (21) has been derived for functions $\tilde{F}_{12/21}$, which are defined by

$$F_{12/21}(\mathbf{k}) = \tilde{F}_{12/21}(\mathbf{k}) \exp \left\{ \pm \frac{2i}{e\mathcal{E}} \int_0^{k_x} dk'_x (J(\mathbf{k}) - \bar{J}(k_y)) \right\}. \quad (23)$$

In Eq. (21), we introduced the quantities

$$d_x^-(l, k_y) = \sum_{l'} Q(l', k_y) d_x(l-l', k_y), \quad d_x^+(l, k_y) = d_x^-(-l, k_y), \quad (24)$$

where

$$Q(l, k_y) = \frac{d}{2\pi} \int_0^{2\pi/d} dk_x e^{-ilk_x d} \times \exp \left\{ - \frac{2i}{e\mathcal{E}} \int_0^{k_x} dk'_x (J(k'_x, k_y) - \bar{J}(k_y)) \right\} \quad (25)$$

and

$$d_x(l, k_y) = - \frac{\alpha^2 m^* \Delta d^2}{4} k_y \frac{d}{2\pi} \int_0^{2\pi/d} dk_x \frac{\cos(lk_x d) \cos(k_x d)}{J^2(k_x, k_y)} = - d(\sqrt{1+c^2}-c)^{|l|}, \quad (26)$$

with $c = 2\hbar^2(k_y d)/(m^* \Delta d)$. It is easily verified that $Q(l, k_y)[d_x(l, k_y)]$ vanishes for odd [even] integers l . A closed equation for $F_z(l, k_y)$ is obtained from Eq. (20), in which the results of the Eqs. (21) and (23) are inserted. To solve these equations, we focus on the pole structure of the solution and collect only those $F_z(l, k_y)$ with a given Wannier-Stark ladder index l . This approximation preserves all qualitative features of the exact result and allows an analytical solution of the form

$$F_z(l, k_y) = \frac{F_z^{(0)}(l, k_y)}{1 + i l \Omega \tau_s + S_l(k_y)}, \quad (27)$$

with

$$S_l(k_y) = 2 \left(\frac{e\mathcal{E}}{\hbar} \right)^2 \tau_s \sum_{l'} \left[\frac{d_x^+(l' - l)^2}{i\Omega l' - 2i\bar{J}(k_y)/\hbar + 1/\tau_s} + \frac{d_x^-(l' - l)^2}{i\Omega l' + 2i\bar{J}(k_y)/\hbar + 1/\tau_s} \right], \quad (28)$$

which is used in Eq. (10) to calculate the magnetization.

IV. THE FIELD-INDUCED MAGNETIZATION

In the Wannier-Stark ladder representation, the magnetization is calculated from Eq. (10) by taking into account Eqs. (27), (28), (21), and (23). We obtain the result

$$f_y = \alpha m^* \frac{\Delta d}{\hbar} \sum_{k_y} \sum_{l=1}^{\infty} B_l(k_y) \Im \{ F_z(l, k_y) \} - 2\alpha e \mathcal{E} \sum_{k_y} \sum_{l_i} \sum_{l=1}^{\infty} k_y A_{l_i - l_2}(k_y) \times \Re \{ [d_x(l_2 - l_3 - l, k_y) R_{l_1, l_2, l_3}(k_y) + d_x(l_2 - l_3 + l, k_y) R_{l_1, l_2, l_3}^*(k_y)] F_z(l, k_y) \}. \quad (29)$$

The first contribution in this equation results from the diagonal elements of the density matrix. It determines the magnetization at low electric fields. The second term describes the impact of the off-diagonal elements on the magnetization and is therefore completely due to quantum effects. The coefficients in Eq. (29) are given by the functions

$$A_l(k_y) = \frac{d}{2\pi} \int_0^{2\pi/d} dk_x \frac{\cos(lk_x d)}{J(k_x, k_y)}, \quad B_l(k_y) = \frac{1}{2}(A_{l-1} - A_{l+1}), \quad (30)$$

$$R_{l_1, l_2, l_3}(k_y) = \frac{Q^*(l_1, k_y) Q(l_3, k_y)}{il_2 \Omega + 2i\bar{J}(k_y)/\hbar + 1/\tau}. \quad (31)$$

The quantities $A_l(k_y)$ and $B_l(k_y)$ are only nonzero for even and odd integer l , respectively.

Our basic result in Eq. (29) simplifies considerably, when the off-diagonal elements of the density matrix $F_{\mu\mu'}$ are not taken into account.¹⁶ Such an approximation is justified under the condition $\hbar/\tau_s < J(k_F)$. In this case, the second term on the right-hand side of Eq. (29) and the quantity $S_l(k_y)$ in the denominator of Eq. (27) disappear, and we obtain

$$f_y = - \alpha m^* \frac{\Delta d}{\hbar} \sum_{l=1}^{\infty} \frac{l \Omega \tau_s}{1 + (l \Omega \tau_s)^2} \sum_{k_y} B_l(k_y) F_z^{(0)}(l, k_y). \quad (32)$$

This equation gives the quasi-classical result for the nonvanishing magnetization in the presence of an electric field. There is a linear field dependence in the Ohmic regime $\Omega \tau_s \ll 1$. The magnetization reaches a maximum around $\Omega \tau_s = 1$ and decreases with increasing electric field according to $f_y \sim 1/\mathcal{E}$. This decrease of the magnetization is due to the Wannier-Stark localization of the electronic states.

Characteristic quantum effects are described by the second term on the right hand side of Eq. (29). The most pronounced quantum corrections are field-induced tunneling resonances that occur at $l\Omega = 2\bar{J}(k_y^*)/\hbar$ for a mean quasi-momentum k_y^* and even integers l . These resonances manifest themselves in the denominator of the quantities $R_{l_1, l_2, l_3}(k_y)$ [see Eq. (31)]. In order to take them into account, we numerically calculate the magnetization from Eq. (29). In Fig. 1, the thick solid line depicts the electric field dependence of f_y for a strongly coupled lateral GaAs/(Al,Ga)As superlattice with a lattice constant of $d=6$ nm, a 2 nm thick barrier and a miniband width of $\Delta=100$ meV. For the sequential tunneling regime in weakly coupled superlattices ($\Delta \rightarrow 0$), the field-induced magnetization disappears. In the Ohmic region, where a linear field dependence is observed, the spin

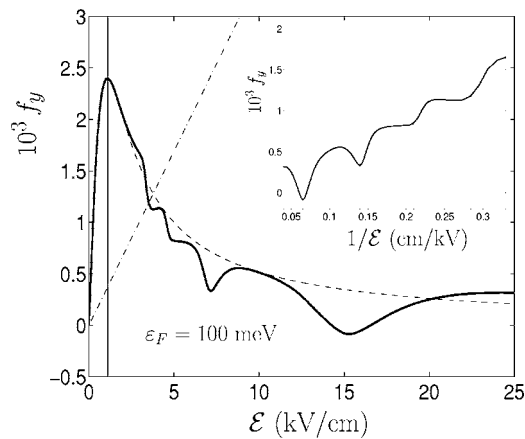


FIG. 1. Spin polarization f_y as a function of the electric field \mathcal{E} for $\varepsilon_F=100$ meV and $\Delta=100$ meV. Other parameters are: $T=4$ K, $d=6$ nm, $\tau=\tau_s=1$ ps, and $\hbar\alpha=5 \times 10^{-9}$ eV cm. The inset shows f_y as a function of $1/\mathcal{E}$. In this representation, the tunneling resonances are equally separated.

polarization is much stronger in superlattices than in the corresponding two-dimensional electron gas [dash-dotted line as calculated from Eq. (13)]. The magnetization reaches a maximum at about $\Omega\tau_s=1$ (vertical solid line) and decreases with increasing electric field according to $f_y \sim 1/\mathcal{E}$. This nonlinear behavior is analytically described by Eq. (32) (dashed line). Field-induced tunneling resonances give rise to minima in the field dependence of the magnetization. These tunneling processes lead to a spin depolarization, whenever different spin states of the biased superlattice are aligned by the electric field.¹⁸ The inset of Fig. 1 shows f_y as a function of $1/\mathcal{E}$. In this representation, the tunneling resonances (marked by vertical solid lines) are equally spaced so that the effective energy gap $2\bar{J}(k_y^*)$ can be estimated.

Note that the spin polarization in the superlattice depends strongly on the ratio between the quasi-Fermi energy ε_F and the miniband width Δ . Figure 2 shows that even the sign of f_y depends on this ratio. The numerical data for Fig. 1 refer to $\varepsilon_F=100$ meV, which gives a positive value for f_y . In Fig. 2, we used $\varepsilon_F=20$ meV and obtained a reversed magnetization f_y . That f_y may change its sign in dependence on the quasi-Fermi energy is related to the fact that the spin polarization is calculated from density matrix elements $F_z(l, k_y)$ with odd integers l . Apart from the change of sign, the details of the lineshape in Fig. 2 agree qualitatively with that in Fig.

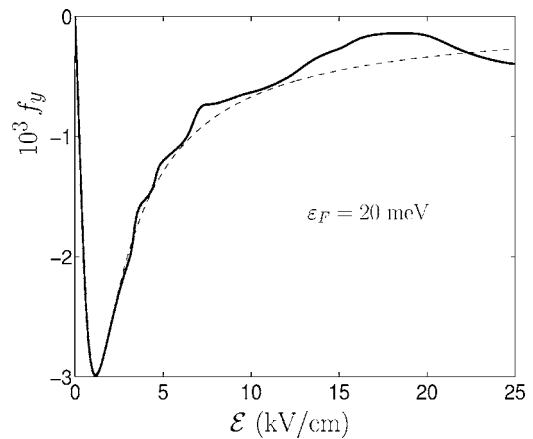


FIG. 2. Spin polarization f_y as a function of the electric field \mathcal{E} for $\varepsilon_F=20$ meV and $\Delta=100$ meV. All other parameters are the same as in Fig. 1.

1. Again the overall line shape of f_y is given by the dashed line calculated from Eq. (32).

V. CONCLUSION

We have generalized the theory of electric-field-induced spin polarization worked out for a two-dimensional electron gas in the linear response regime⁷ to strongly coupled lateral superlattices in the high-field regime, where Wannier-Stark localization takes place. We have shown that a constant electric field applied parallel to a superlattice induces an in-plane magnetization. In the linear field regime, the effect is much larger than in the related two-dimensional electron gas. The spin polarization reaches a maximum at about $\Omega\tau_s=1$ and decreases with increasing electric field according to $f_y \sim 1/\mathcal{E}$. Tunneling resonances between different spin states lead to a spin depolarization. The magnitude of the field-induced spin polarization is small ($f_y < 1\%$ in the parameter range studied here). Nevertheless, its experimental demonstration seems to be possible for lateral superlattices fabricated by the cleave edged overgrowth technique.

ACKNOWLEDGMENT

Partial financial support by the Deutsche Forschungsgemeinschaft is gratefully acknowledged.

¹J. E. Hirsch, Phys. Rev. Lett. **83**, 1834 (1999).

²R. V. Shchelushkin and Arne Brataas, Phys. Rev. B **71**, 045123 (2005).

³Y. K. Kato, R. C. Myers, A. C. Gossard, D. D. Awschalom, Science **306**, 1910 (2004).

⁴J. Sinova, D. Culcer, Q. Niu, N. A. Sinitsyn, T. Jungwirth, and A. H. MacDonald, Phys. Rev. Lett. **92**, 126603 (2004).

⁵S. Murakami, N. Nagaosa, and S. C. Zhang, Science **301**, 1348 (2003).

⁶K. Nomura, J. Sinova, T. Jungwirth, Q. Niu, and A. H. MacDonald, Phys. Rev. B **71**, 041304(R) (2005).

⁷V. M. Edelstein, Solid State Commun. **73**, 233 (1990).

⁸A. G. Aronov, Yu. B. Lyanda-Geller, and G. E. Pikus, Zh. Eksp. Teor. Fiz. **100**, 973 (1991) [Sov. Phys. JETP **73**, 537 (1991)].

⁹E. G. Mishchenko, A. V. Shytov, and B. I. Halperin, Phys. Rev. Lett. **93**, 226602 (2004).

¹⁰J. I. Inoue, G. E. W. Bauer, and L. W. Molenkamp, Phys. Rev. B **67**, 033104 (2003).

- ¹¹O. Bleibaum, Phys. Rev. B **71**, 195329 (2005).
- ¹²S. D. Ganichev, S. N. Danilov, P. Schneider, V. V. Bel'kov, L. E. Golub, W. Wegscheider, D. Weiss, and W. Prettl, cond-mat/0403641 (unpublished).
- ¹³Y. K. Kato, R. C. Myers, A. C. Gossard, and D. D. Awschalom, Phys. Rev. Lett. **93**, 176601 (2004).
- ¹⁴S. D. Ganichev, E. L. Ivchenko, V. V. Bel'kov, S. A. Tarasenko, M. Sollinger, D. Weiss, W. Wegscheider, and W. Prettl, Nature (London) **417**, 153 (2002).
- ¹⁵V. V. Bryksin, V. C. Woloschin, and A. W. Rajtzev, Fiz. Tverd. Tela (Leningrad) **22**, 3076 (1980) [Sov. Phys. Solid State **22**, 1796 (1980)].
- ¹⁶P. Kleinert and V. V. Bryksin, Phys. Rev. B **72**, 153103 (2005).
- ¹⁷V. V. Bryksin and Y. A. Firsov, Zh. Eksp. Teor. Fiz. **61**, 2373 (1971) [Sov. Phys. JETP **34**, 1272 (1971)].
- ¹⁸P. Kleinert and V. V. Bryksin, J. Phys.: Condens. Matter **17**, 3865 (2005).